ISSN (Print) : 2320 – 3765
ISSN (Online): 2278 – 8875

International Journal of Advanced Research in Electrical, Electronics and Instrumentation Engineering

(An ISO 3297: 2007 Certified Organization)

Vol. 2, Issue 8, August 2013

Simulation of I-F Starting of PMSM Drive

Sonia Thomas[1], Dominic Mathew[2]

M.Tech Scholar, Dept of EEE, Rajagiri School of Engineering and Technology,Cochin,India[1]

Professor, Dept of AEI, Rajagiri School of Engineering and Technology,Cochin,India[2]

ABSTRACT: This paper proposes a new I-f starting method based on closed-loop current regulation for sensor less back EMF based FOC of PMSM drive. A new transition process is introduced before switching from the start up strategy to the sensor less FOC strategy. This transition period ensures a smooth switching from starting to back -EMF-based sensor less FOC algorithm. The method proposed in this paper is simple and can work with different load situations. The performance of this start up process is also robust under different motor parameter variations.Detailed analysis of I-F starting is given.The new start up method is validated using simulation results done in MATLAB/Simulink on a 480V, 2850rpm PMSM motor

KEYWORDS: PMSM DRIVE, I-F STARTING, FOC

1. INTRODUCTION

In the last years the induction machine has been a nice solution for applications but PMSM motor has become a very important competitor because of the high efficiency. The most easiest and frequent method to estimate the position of the rotor is the one based on back Electromotive force (EMF). In this strategy the variables necessary to compute the back EMF are estimated from the electrical parameter of the machines. The mechanical components are deducted from the estimated values from the back EMF.The back-EMF-based method is usually operated in medium and high-speed range. It suffers from weak back EMF signals during this speed range. An additional start up procedure is required for high speed applications.

A new start up method is introduced here which ensures that the drive is able to accelerate to a speed at which the back-EMF is high enough to be accurately sensed. The absence of current regulation may cause high current and torque ripples during the transition from the start up stage to the FOC stage, which also increases the risk that FOC may not be switched in successfully. To overcome these problems, closed-loop control strategies should be adopted. This *I–f* starting method appears to be a better solution Instead of specifying a voltage reference used in the *V/f* control, the current in the *I–f* control is specified and maintained constant in a synchronous rotating reference frame. The motor is accelerated by following a ramping up frequency command.

II. STARTUP PROCEDURE

As known the back-EMF sensor less algorithm has the disadvantage of disability in very low speed, the motor cannot start up successfully by this algorithm. To overcome the drawback, an open-loop start up strategy is introduced. The rotor can be dragged by predetermined voltages to a certain speed and shift to sensor less algorithm automatically with low torque impact.

There are several methods to determine the voltages, one of which is to give 3-phase sinusoidal voltages directly, with the amplitude related to the frequency of sinusoidal waves, so called V/F open-loop control. This strategy has been tested in lab and the result is not so satisfactory. Because it is a complete open-loop without any feedbacks from current and voltage sensors, the amplitude of voltages are difficult to determine, especially in both with or without load conditions. Usually those uncontrollable voltages generate large currents in stator while the power factor is quite low. Furthermore, low efficiency currents make magnetization in d axis so that the inductance L_d may be affected. That may lead to estimation inaccuracy. Therefore, another half-closed-loop strategy is chosen, which has better performance than that of the V/F open-loop control.

ISSN (Print) : 2320 – 3765
ISSN (Online): 2278 – 8875

International Journal of Advanced Research in Electrical, Electronics and Instrumentation Engineering

(ISO 3297: 2007 Certified Organization)

Vol. 2, Issue 8, August 2013

III. HALF-CLOSE-LOOP STRATEGY

In this experiment, the start-up procedure has closed current loop and open speed loop. That means both the i_d and i_q are self-adjusted by PI control. However the speed cannot be fed back because it is impossible to get precise speed at low speed. Figure 5.1 shows the topology that the reference i_q is given by default value and locked by current loop. During start up process, the reference angle and speed are generated by ramping in low speed condition, shown as the θ Generator. If speed reaches a certain value and both the estimated speed and angle are precise enough, the switches of θ and i_q shift successively, from position 1 to position 2 shown below

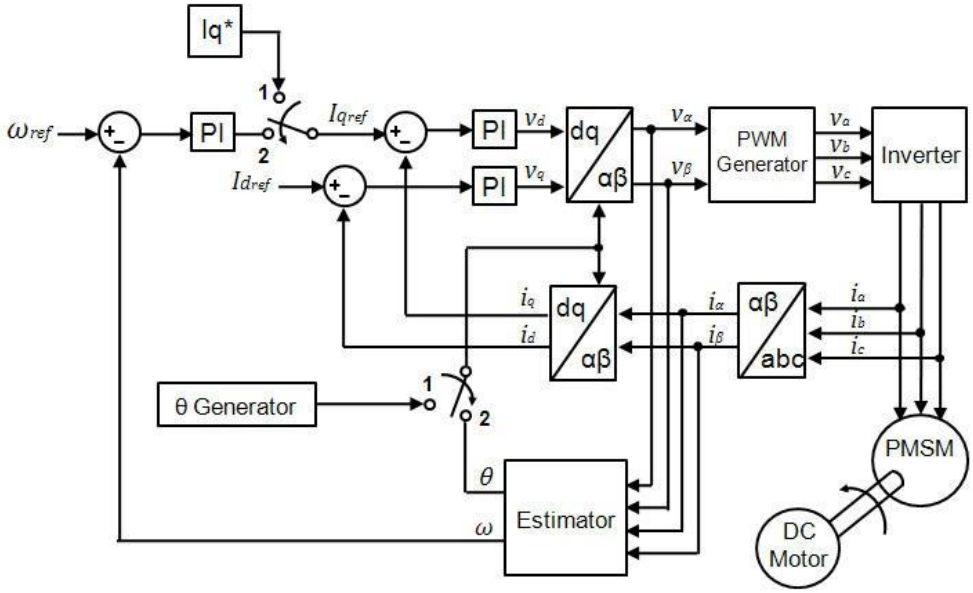

Figure 1. Vector control scheme with start-up procedure

IV. STRATEGY CONVERSION

The key point of start-up procedure is to make conversion smooth in different conditions. To make the rotor accelerate smoothly, an angular velocity is given and it increases slowly by ramping, the angle is achieved by time integration, which can be described as:

$$\omega = \int \Delta\omega dt, where \Delta\omega = const \qquad (1)$$

A new coordinate named dq* is introduced here, whose d axis is in phase with the given angle θ. The figure 2 gives the phasor diagram.

ISSN (Print) : 2320 – 3765
ISSN (Online): 2278 – 8875

International Journal of Advanced Research in Electrical, Electronics and Instrumentation Engineering

(ISO 3297: 2007 Certified Organization)

Vol. 2, Issue 8, August 2013

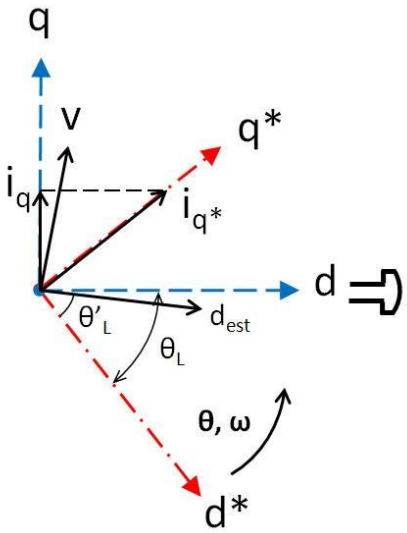

Figure 2. Phasor diagram in dq and dq* axes

In this coordinate i_d is still supposed to be 0 and i_q is supposed to be a constant i_q^* , which aligns with the q*-axis. At the beginning of start-up, the d* is set to -90°lag in phase with real d-axis so that the rotor can start to move very smoothly. The lagging angle between d* and d-axes is defined as θ_L :

$$\theta_L = \theta^* - \theta_{est} \qquad (2)$$

As rotor speeding up, the θ_L tends to be a definite value depending on the fixed load and acceleration. At the same time, the back-EMF sensor less algorithm calculates the rotor angle as well. However the estimated angle is not quite accurate at this moment, as *dest* shown in Figure 2, because the L_d is affected by magnetization of d component of i_q^* due to flux saturation in d axis. It may be difficult to estimate saturation of the stator flux or make proper compensation for L_d , so in this condition status conversion may not be stable. To overcome this problem, an i_q self-adjustment procedure is introduced in order to improve the estimation accuracy and make the status conversion smooth. The main idea is to reduce i_q to a proper value so that the current vector i_q^* keeps the angle of 90 degrees with d-axis, as explained in equation (3) to (5). It can be deduced that a new value i_q' can satisfied the torque at condition of θ_L = 0, which means there is no phase lag between d* and d axes.

$$T = \frac{3}{2} p i_q \Psi_d = \frac{3}{2} p i_q^* \cos\theta_L \left(\Psi_{mpm} + L_d i_q^* \sin\theta_L\right)$$

$$T - T_L = J\frac{d\omega}{dt} = J\Delta\omega \qquad (3),(4),(5)$$

$$T = T_L = \frac{3}{2} p i_q^* \cos\theta_L \left(\Psi_{mpm} + L_d i_q^* \sin\theta_L\right)$$

$$= \frac{3}{2} p i_q' \Psi_{mpm}$$

ISSN (Print) : 2320 – 3765
ISSN (Online): 2278 – 8875

International Journal of Advanced Research in Electrical, Electronics and Instrumentation Engineering

(ISO 3297: 2007 Certified Organization)

Vol. 2, Issue 8, August 2013

From equation (5), the expected value can be solved

$$i_q^{'} = i_q^{*} \cos\theta_L \left(1 + \frac{L_d i_q^{*} \sin\theta_L}{\Psi_{mpm}}\right) \qquad (6)$$

The equation (6) gives the result of adjusted i_q' . The next step is to reduce i_q from i_q^* to i_q' . The θ_L closed loop starts to work during conversion process, as shown in Figure 3. By comparing the present θ_L and expectant θ_{L_ref} , the error $\Delta\theta_L$ then goes through a regulator. The output is the reference i_q^* which tracks the $\Delta\theta_L$ to be zero. It is not recommended to drop i_q too fast since the speed could be unstable in dynamic transition. During the reduction of i_q , a new torque balance establishes and the d*-axis tends to be aligned with real d-axis, as well as the estimated rotor position *dest*. Finally the estimated position *dest* replaces the given coordinate d*, the speed loop starts working instead of loop, as shown in Figure 3.The advantage of the i_q self-adjustment procedure is that the current during start-up never exceeds too much and more significantly, it could response to the load variation. No matter with or without load, status conversion always operates successfully and smoothly. For better understanding of this procedure, the whole process can also be recognized as a θ closed loop outside the i_q loop, shown as the following flowchart:

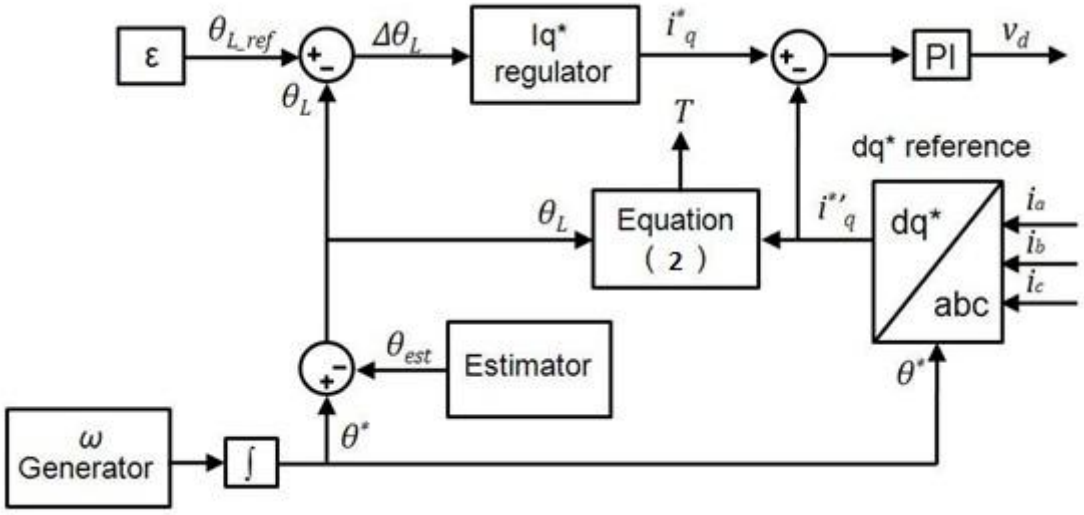

Figure 3. Scheme of adjustment procedure

In summary, the start-up procedure can be divided into following five steps:

1) By injecting DC current as shown in Figure, the rotor is aligned with the initial angle position.

2) The rotor angle θ and the reference i_q are given directly and the speed increases continuously with a smooth slope. The estimator operates not so well in very low speed and becomes better during speedup.

3) When the speed approaches to the threshold speed ω_{thred} , an i_q adjustment procedure is taken into effect and the i_q decreases gradually with a slope. At this moment the θ_{est} from estimator is getting more and more accurate.

4) If the estimated field angle θ_{est} is accurate enough, it replaces the given rotor angle, and the reference i_q is shifted and generated by speed loop.

5) The motor runs in sensor less vector control, accelerates rapidly to final speed and then keeps running at uniform speed.

ISSN (Print) : 2320 – 3765
ISSN (Online): 2278 – 8875

International Journal of Advanced Research in Electrical, Electronics and Instrumentation Engineering

(ISO 3297: 2007 Certified Organization)

Vol. 2, Issue 8, August 2013

V. VECTOR CONTROL

Field Oriented Control (FOC) is one of the most used technique for controlling the torque of a permanent magnet synchronous motor. For a simpler implementation the strategy is using the synchronous reference frame. FOC is a close loop strategy and is composed by two current controllers necessary for controlling the torque and one speed controller. The controllers are PI's (Proportional Integrator) due to theirs good steady state errors.

The measurement values necessary in the control are the DC voltage, the three phase stator current and the rotor position of PMSM. The integration of the speed will give the rotor position, necessary in the transformation of the measured stator currents into dq reference frame axis. The d and q current component are the feedback currents for the current controllers. The speed controller generates the torque that will command the reference frame currents is $i_{dref}{}^{s}$ and $i_{qref}{}^{s}$ is from this torque command the reference currents $i_{qref}{}^{s}, i_{qref}{}^{s}$ are set based on the control strategies presented in details further on. The reference currents are compared with the actual rotor currents in the dq reference frame and send to two current controllers. The output of the controllers represents the required dq voltages. To control the current independently one of each other is necessary to add the compensation term $\omega_e \lambda_d{}^{s}$ and to subtract $\omega_e \lambda_q{}^{s}$ term from the output of the current controllers. The dq components of the voltage are transform to $\alpha\beta$ reference frame in order to compute the duty cycles necessary in Space Vector Modulation strategy. Finally the PWM generator block calculates the switching signals for the inverter.

VI. ROTOR POSITION ESTIMATION

Now we continue to deduce the voltage equations of PMSM, by giving the restrictive conditions in stationary αβ reference frame, where $\hat{\theta} = \theta_r$ and ω =0.

$$\begin{bmatrix} V_\alpha \\ V_\beta \end{bmatrix} = \begin{bmatrix} R_s & 0 \\ 0 & R_s \end{bmatrix} \begin{bmatrix} i_\alpha \\ i_\beta \end{bmatrix} + \frac{d}{dt} \begin{bmatrix} \Psi_\alpha \\ \Psi_\beta \end{bmatrix} \quad (7)$$

Where

$$\begin{bmatrix} \Psi_\alpha \\ \Psi_\beta \end{bmatrix} = \begin{bmatrix} L_1 + L_2 \cos 2\theta_r & L_2 \sin 2\theta_r \\ L_2 \sin 2\theta_r & L_1 - L_2 \cos 2\theta_r \end{bmatrix} \begin{bmatrix} i_\alpha \\ i_\beta \end{bmatrix} + \begin{bmatrix} \cos\theta_r \\ \sin\theta_r \end{bmatrix} \Psi_{PM} \quad (8)$$

The equation (8) can be arranged in the form:

$$\Psi_\alpha - L_1 i_\alpha = \Psi_{PM} \cos\theta_r + L_2 \left(i_\alpha \cos 2\theta_r + i_\beta \sin 2\theta_r \right)$$
$$\Psi_\beta - L_1 i_\beta = \Psi_{PM} \sin\theta_r + L_2 \left(i_\alpha \sin 2\theta_r - i_\beta \cos 2\theta_r \right) \quad (9),(10)$$

Define space vectors in complex coordinate:

$$\bar{Z}_1 \triangleq \left(\Psi_\alpha - L_1 i_\alpha \right) + j \left(\Psi_\beta - L_1 i_\beta \right)$$
$$\bar{Z}_2 \triangleq \Psi_{PM} \left(\cos\theta_r + j \sin\theta_r \right) = \Psi_{PM} e^{j\theta_r}$$
$$\bar{Z}_1 = \bar{Z}_2 + \bar{Z}_3$$
$$\bar{Z}_3 \triangleq L_2 \left[\left(i_\alpha \cos 2\theta_r + i_\beta \sin 2\theta_r \right) + \left(i_\alpha \sin 2\theta_r - i_\beta \cos 2\theta_r \right) \right] \quad (11), (12), (13)$$
$$\bar{I} \triangleq I_s e^{j\theta_i} = \left(i_\alpha + j i_\beta \right) \quad (14), (15)$$

From equation (13) it can be seen that the vector $\bar{Z}_2$ is constrained in a circle with the radius of Ψ_{PM} , and has the space angle of θ_r similarly, when $\bar{Z}_3$ is further deduced as:

ISSN (Print) : 2320 – 3765
ISSN (Online): 2278 – 8875

International Journal of Advanced Research in Electrical, Electronics and Instrumentation Engineering

(ISO 3297: 2007 Certified Organization)

Vol. 2, Issue 8, August 2013

$$\left[\mathrm{Re}\left(\vec{Z}_3\right)\right]^2+\left[\mathrm{Im}\left(\vec{Z}_3\right)\right]^2=L_2{}^2\left(i_\alpha{}^2+i_\beta{}^2\right)=L_2{}^2I_s{}^2 \qquad (16)$$

It can be seen that the vector $\vec{Z}_3$ is constrained in another circle, with the radius of L_2I_s .As a result, it is not difficult to show the graphical interpretation in Fig. 4, where $\theta_1,\theta_2,\theta_3$ are the angles of those relative vectors.

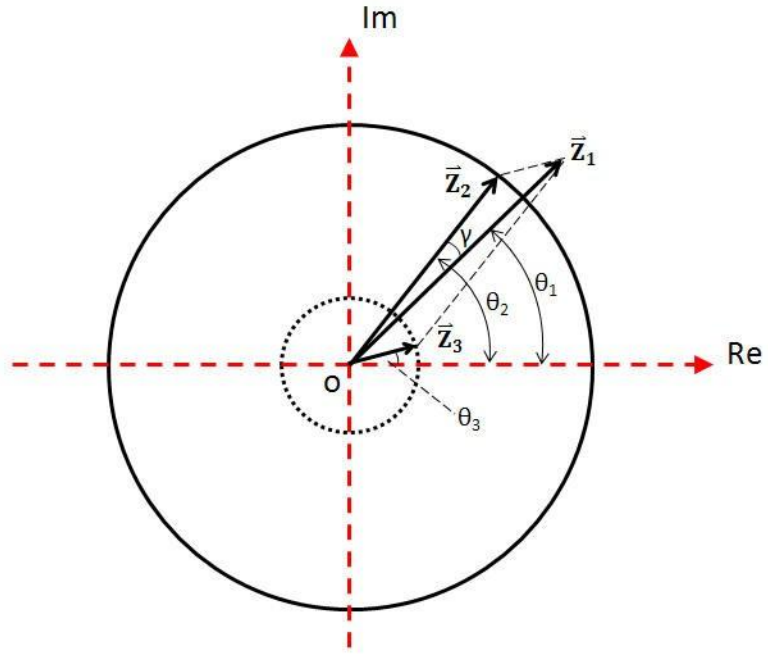

Figure 4. Graphical interpretation of space vector

The angles of those vectors are

$$\theta_1=\arg\left(\vec{Z}_1\right)=\tan^{-1}\frac{\Psi_\beta-L_1i_\beta}{\Psi_\alpha-L_1i_\alpha}$$

$$\theta_2=\arg\left(\vec{Z}_2\right)=\theta_r$$

$$\theta_3=\arg\left(\vec{Z}_3\right) \qquad (17),(18),(19)$$

$$=\arg\left[L_2\left(i_\alpha-ji_\beta\right)\left(\cos2\theta_r+j\sin2\theta_r\right)\right]$$

$$=\arg\left[L_2I_se^{j(2\theta_r-\theta_i)}\right]$$

$$=2\theta_r-\theta_i$$

Considering about the triangle $\Delta0Z_1Z_2$, which is composed of vectors $\vec{Z}_1,\vec{Z}_2,\vec{Z}_3$, the angle γ is

$$\gamma=\cos^{-1}\left[\frac{\left|\vec{Z}_1\right|^2+\left|\vec{Z}_2\right|^2-\left|\vec{Z}_3\right|^2}{2\left|\vec{Z}_1\right|\left|\vec{Z}_2\right|}\right] \qquad (20)$$

Thus, the rotor position can finally achieved by geometry calculation

$$\theta_r=\theta_2=\theta_1+\gamma \qquad (21)$$

ISSN (Print) : 2320 – 3765
ISSN (Online): 2278 – 8875

International Journal of Advanced Research in Electrical, Electronics and Instrumentation Engineering

(ISO 3297: 2007 Certified Organization)

Vol. 2, Issue 8, August 2013

Before the conclusion being stated, one thing should be proved, that is the position relationship between vector $\vec{Z}_2$ and $\vec{Z}_3$. As shown in Fig.4, the (angle of $\vec{Z}_2$) goes ahead of (angle of $\vec{Z}_3$ **)**. The further explanation is illustrated as follows

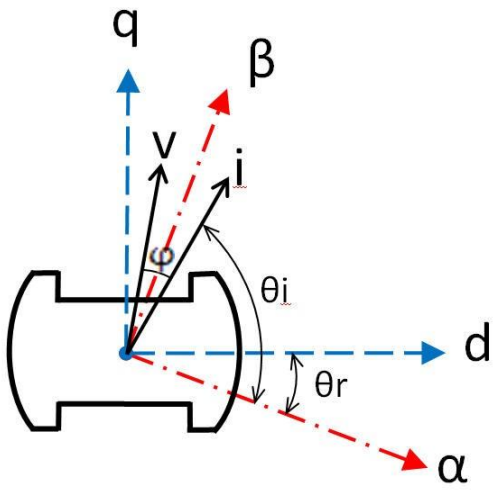

Figure 5.Space-time phasor diagram of synchronous motor

According to the Figure 5, we can find that in condition of i_q not equal to zero, which means if it works in motor state with power output onto the shaft, the rotor position always lags the vector $\vec{I}$, that is $\theta_i \rangle \theta_r$. So the comparison of and may be deduced as

$$\theta_2 - \theta_3 = \theta_r - (2\theta_r - \theta_i) = \theta_i - \theta_r > 0 \qquad (22)$$

The comparison result is $\theta_2 > \theta_3$, which means that Z_2 always leads $\vec{Z}_3$.

VII. ALGORITHM IMPLEMENTATION

The inputs are stator voltages and currents in reference frame, and the output is the estimated field angle representing the current rotor position with respect to stator phase A. In most cases, for surface mounted PM, the difference between L_d and L_q is not remarkable, L_2 is a small value. Thus, the magnitude of vector $\vec{Z}_3$ is far smaller compared to vectors $\vec{Z}_1$ and $\vec{Z}_2$, so that the angle γ is quite small as well. The inductance L_d and L_q may be replaced by a common inductance L_1 , and the equation (29) could be simplified as $\theta_r \approx \theta_1$, where the error of γ may be omitted during calculation. However, this is a universal algorithm for both salient and non-salient PM motors. For inner mounted PM with remarkable difference between L_d and L_q , the universal method gives better results than conventional back-EMF methods.

ISSN (Print) : 2320 – 3765
ISSN (Online): 2278 – 8875

International Journal of Advanced Research in Electrical, Electronics and Instrumentation Engineering

(ISO 3297: 2007 Certified Organization)

Vol. 2, Issue 8, August 2013

VIII. SIMULATION BLOCKS

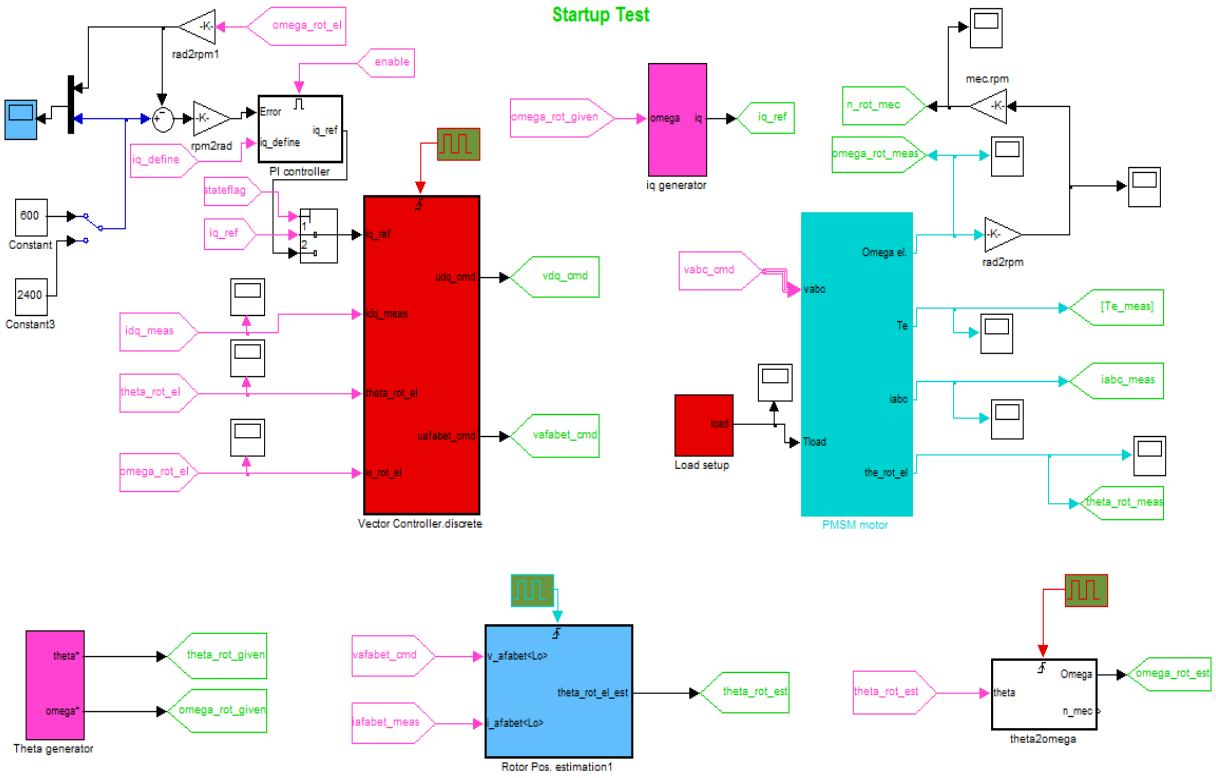

Figure 6. Simulation diagram of I-F starting of PMSM drive

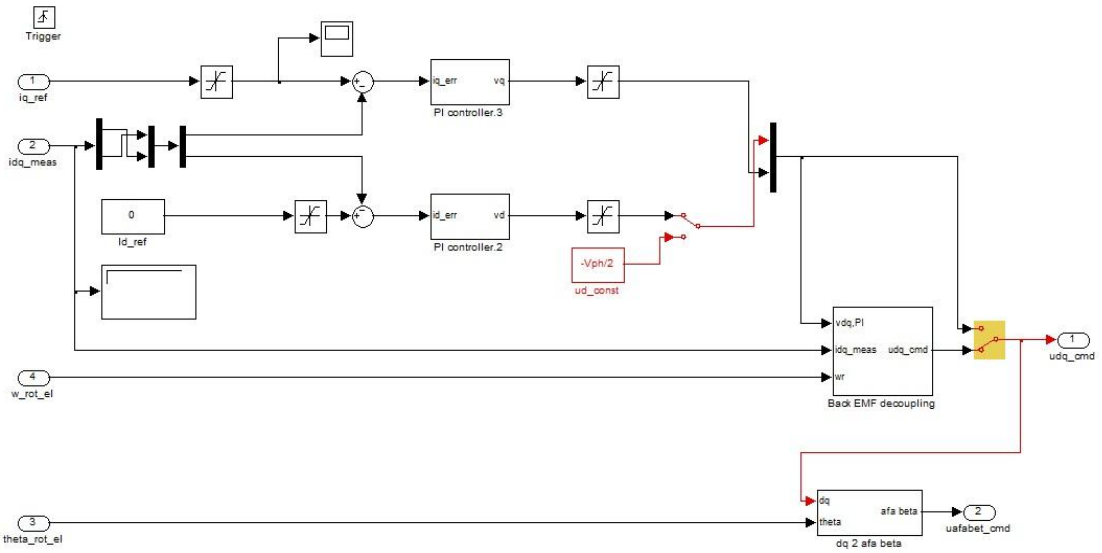

Figure 7. Simulation diagram of Vector Control

ISSN (Print) : 2320 – 3765
ISSN (Online): 2278 – 8875

International Journal of Advanced Research in Electrical, Electronics and Instrumentation Engineering

(ISO 3297: 2007 Certified Organization)

Vol. 2, Issue 8, August 2013

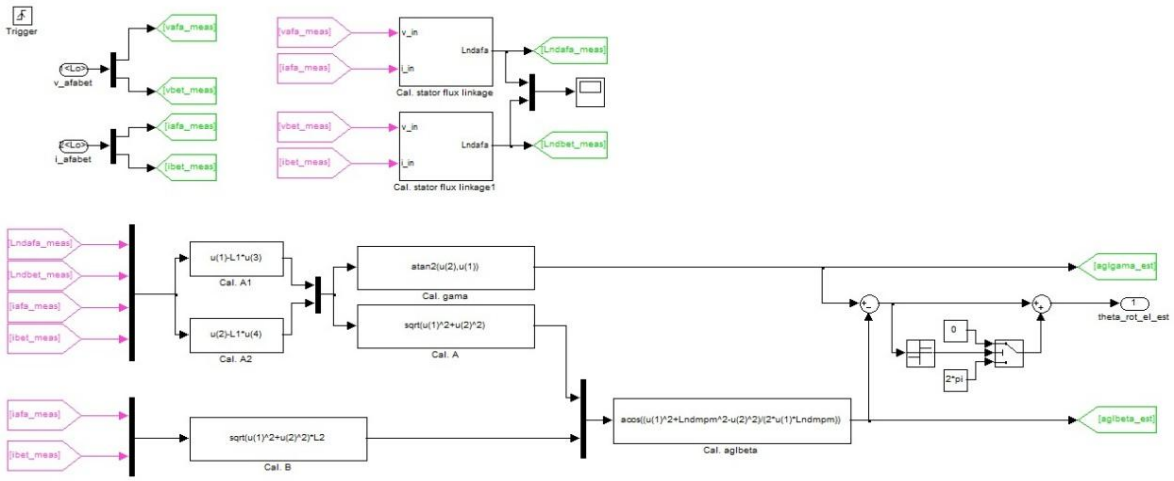

Figure 8. Simulation diagram of Rotor Position Estimation

IX. SIMULATION RESULTS

The simulation results are obtained by solving nonlinear equations using MATLAB. For this I-F starting process model, the PWM generator and inverter are not included. By directly connecting command stator voltages to the motor, the PWM generation and inverter are neglected to simplify the iteration loop, so that to speed up the calculation. The difference between ideal alpha-beta command voltage in simulation and real voltage generated by inverter is the waveform distortion caused by dead –band of PWM signals. Another difference is the time delay. For real use of this algorithm, the time delay caused by DSP's PWM shadow function has to be complemented, while in simulation there is no such problem.

The state flag used in the simulation is controlled by erroneous angle between assigned ramping angle and algorithm estimated angle. If they coincide, the flag shifts.

TABLE I
MOTOR PARAMETERS

Stator Resistance	2.35 Ω
d-axis inductance	10mH
q-axis inductance	15.4mH
Pole Pairs	2
Rated Speed	2850rpm
Rated Power	470W

ISSN (Print) : 2320 – 3765
ISSN (Online): 2278 – 8875

International Journal of Advanced Research in Electrical, Electronics and Instrumentation Engineering

(ISO 3297: 2007 Certified Organization)

Vol. 2, Issue 8, August 2013

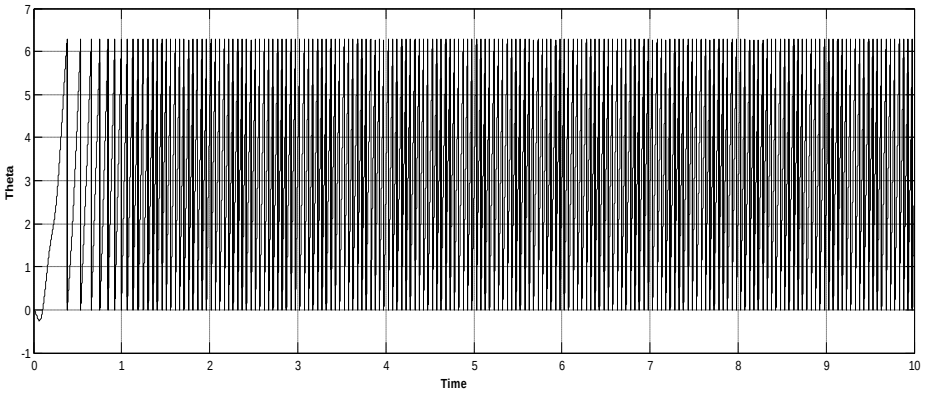

Figure 9.Theta measured from PMSM motor

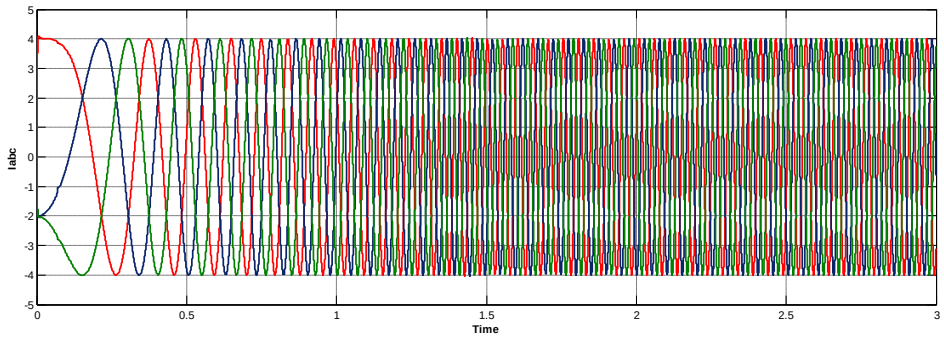

Figure 10.Stator currents of PMSM

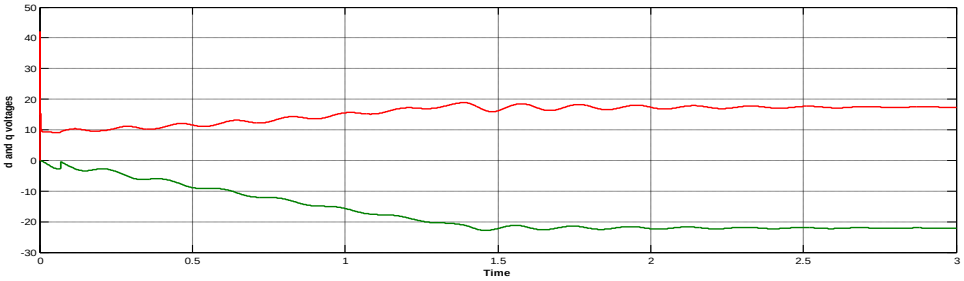

Figure 11. d and q voltages

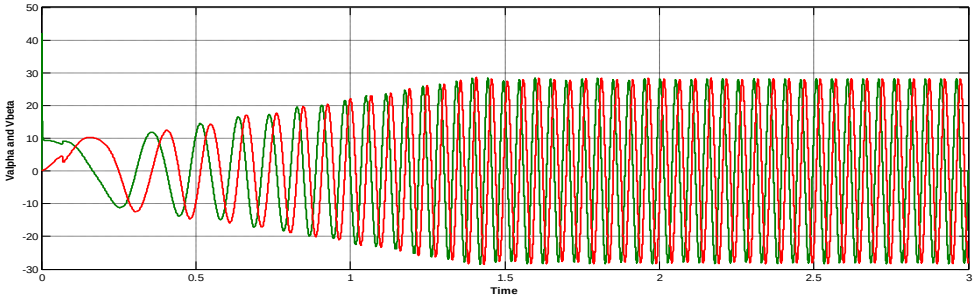

Figure 12.Alpha and beta voltages

ISSN (Print) : 2320 – 3765
ISSN (Online): 2278 – 8875

International Journal of Advanced Research in Electrical, Electronics and Instrumentation Engineering

(ISO 3297: 2007 Certified Organization)

Vol. 2, Issue 8, August 2013

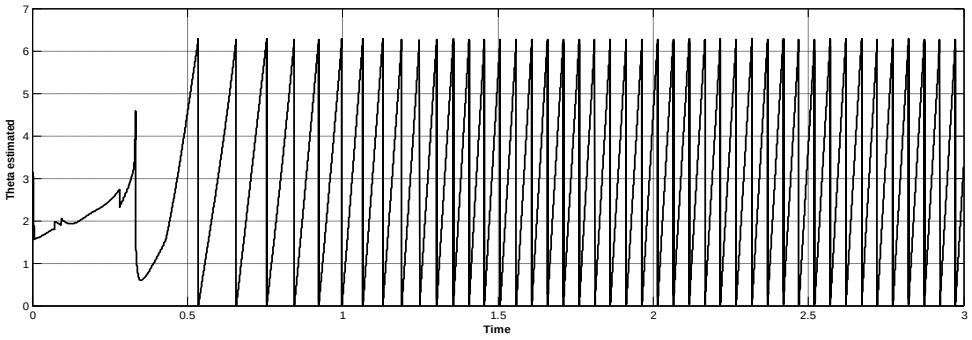

Figure 13.Theta estimated using position estimation block

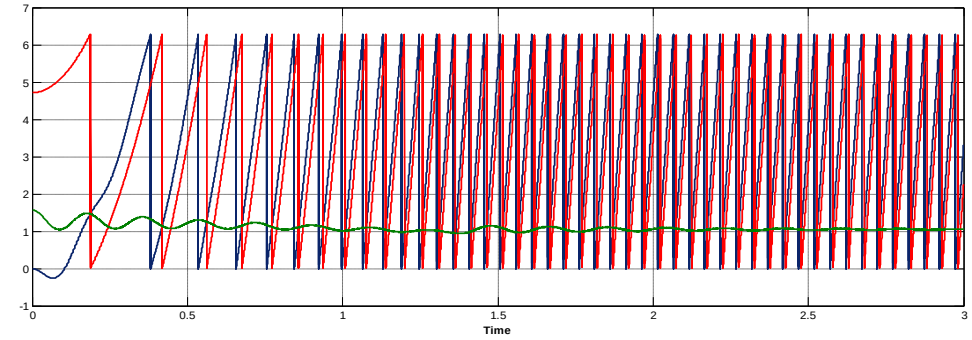

Figure 14. Measured theta from motor, estimated theta and transient behaviour of theta during starting

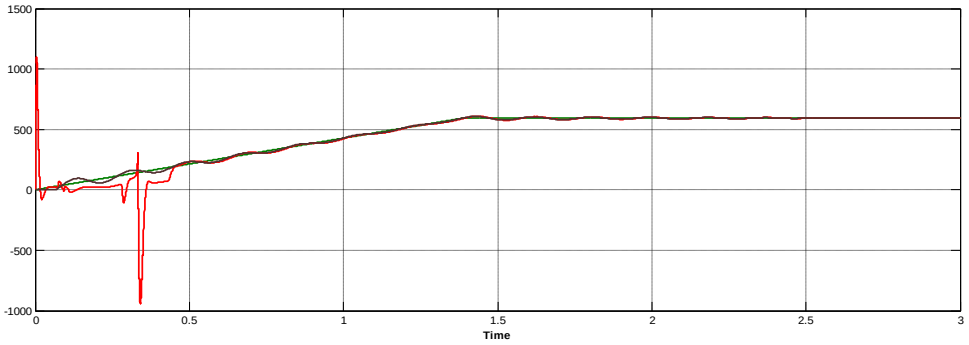

Figure 15. Measured shaft speed from motor. Estimated speed and nature of speed during starting

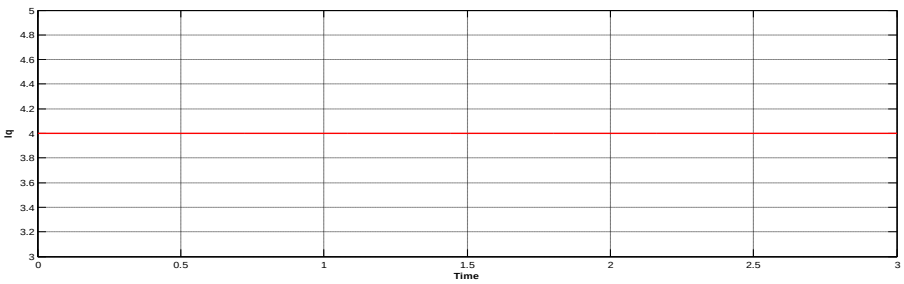

Figure 16. Reference Iq used for start-up process

ISSN (Print) : 2320 – 3765
ISSN (Online): 2278 – 8875

International Journal of Advanced Research in Electrical, Electronics and Instrumentation Engineering

(ISO 3297: 2007 Certified Organization)

Vol. 2, Issue 8, August 2013

X. CONCLUSION

In this paper, I-F starting method based on current regulation is introduced for back EMF base sensor less field oriented control of PMSM. This starting method controls synchronous rotating frame current components in the starting stage and matches it with values generated in the FOC stage. This starting method is robust and can work under different load conditions. Torque and current ripples are considerably get reduced during transition from start-up stage up to FOC stage. Detailed analysis of start-up method is given and validated using MATLAB simulation.

REFERENCES

[1]. F. Genduso, R. Miceli, C. Rando, and G. R. Galluzzo, "Back EMF sensor less-control algorithm for high-dynamic performance PMSM,"*IEEE Trans. Ind. Electron.*, vol. 57, no. 6, pp. 2092–2100, Jun. 2010

[2]. B. N. Mobarakeh, F. Meibody-Tabar, and F.-M. Sargos, "Back-EMF estimation based sensor less control of PMSM: Robustness with respect to measurement errors and inverter irregularities," in *Conf. Rec. 39th IEEE IAS Annu. Meet.* 2004, vol. 3, pp. 1858–1865.

[3]. M. Fatu, R. Teodorescu, I. Boldea, and G. D. Andreescu, "I-F starting method with smooth transition to EMF based motion-sensorless vector control of PM synchronous motor/generator," in in *Conf. Rec. Power Electron. Spec. Conf.*, 2008, pp. 1481–1487.

[4]. A. Stirban, I. Boldea, G.-D. Andreescu, D. Iles, and F. Blaabjerg, "Motion sensorless control of BLDC Motor with offline FEM info assisted state observer," in *12th Int. Conf. OPTIM*, 2010, pp. 321–328

BIOGRAPHY

Sonia Thomas received her B-TECH degree in Electrical and Electronics engineering from Rajagiri School of Engineering and Technology, Ernakulum, India in 2011, where she is currently working towards Master's degree.

Her areas or interest are sensor less control algorithms of permanent magnet synchronous motor drives and its control